

**Research Article**

## PAPR reduction using selective mapping scheme in universal filtered multicarrier waveform

Şakir Şimşir <sup>a,\*</sup>  and Necmi Taşpınar <sup>b</sup> 

<sup>a</sup>Nevşehir Hacı Bektaş Veli University, Department of Electrical and Electronics Engineering, Nevşehir, 50300, Turkey

<sup>b</sup>Erciyes University, Department of Electrical and Electronics Engineering, Kayseri, 38039, Turkey

**ARTICLE INFO***Article history:*

Received 30 April 2020

Revised 31 May 2020

Accepted 06 July 2020

*Keywords:*

Peak to average power ratio

Selective mapping

Solid state power amplifier

Universal filtered multicarrier

5G

**ABSTRACT**

In this paper, the selective mapping (SLM) technique possessing the powerful and distortionless peak to average power ratio (PAPR) reduction capability was employed in universal filtered multicarrier (UFMC) waveform that is considered as one of the most promising fifth generation (5G) waveform candidates in order to provide a solution to the PAPR issue encountered in the related waveform. Owing to our SLM-based PAPR reduction implementation performed by employing the SLM scheme between the quadrature amplitude modulation (QAM) mapping and bandwidth-subdivision operations at the transmitter side, successful PAPR reduction results were achieved in a straightforward and effective manner. In the simulations, the effect of the related way of SLM application on alleviating the PAPR and spectral leakages of the UFMC signal amplified via the solid state power amplifier (SSPA) was investigated for various number of phase factor combinations. Besides, the impact of SLM on the bit error rate (BER) of the UFMC waveform was analyzed for varied values of SSPA parameters called smoothness ( $p$ ) and input back off (IBO) controlling the linearity and operation point of the SSPA, respectively.

© 2020, Advanced Researches and Engineering Journal (IAREJ) and the Author(s).

**1. Introduction**

Universal filtered multicarrier (UFMC) [1] is a newly proposed waveform having the potential to replace the conventional orthogonal frequency division multiplexing (OFDM) which is unable to provide the next generation telecommunication standards. The disadvantages such as the requirement of synchronization, sensitivity to frequency offsets and the problem of high side lobes posing a real obstacle for OFDM to be employed in the fifth generation (5G) systems were successfully resolved by the UFMC while maintaining the key features of the conventional OFDM. In the UFMC scheme, the whole bandwidth is divided into multiple sub-bands to be filtered, fragmentally. Thanks to the filtering per sub-band operation, it is possible to use low length filters making the UFMC suitable for short burst communication. Moreover, the out of band (OOB) radiation which makes any waveform vulnerable to the problem of inter carrier interference (ICI), can be alleviated significantly by the UFMC scheme. Having the low side lobes enhances the

suitability of UFMC waveform to be used in the fragmented spectrum. As well as these superior features, possessing the fundamental OFDM features makes the UFMC waveform quite flexible to be used in multiple services [2-4].

Due to the fact that UFMC is a kind of waveform using multicarrier transmission strategy as the OFDM waveform, the aforementioned superior features don't prevent the UFMC from being exposed to the high peak to average power ratio (PAPR) problem. As known, a nonlinear high power amplifier (HPA) is employed at the transmitter end in order to amplify the signals prior to the transmission process and such amplifiers which are preferred in real applications cannot perform a healthy amplification out of a certain range. Therefore, the high PAPR signals which push the related type of amplifiers to exceed the linear amplification range and reach to the saturation region cannot be amplified without any degradation which results in the increase of both OOB radiation and bit error rate (BER). In order to minimize

\* Corresponding author. Tel.: +90 (384) 228 1000 - 15066; Fax: +90 (384) 228 11 23.

E-mail addresses: [sakirsimsir@nevsehir.edu.tr](mailto:sakirsimsir@nevsehir.edu.tr) (Ş. Şimşir), [taspinar@erciyes.edu.tr](mailto:taspinar@erciyes.edu.tr) (N. Taşpınar)

ORCID: 0000-0002-1287-160X (Ş. Şimşir), 0000-0003-4689-4487 (N. Taşpınar)

DOI: 10.35860/iarej.730126

such signal distortions, many type of PAPR reduction algorithms such as tone injection (TI) [5], active constellation extension (ACE) [6], selective mapping (SLM) [7, 8], tone reservation (TR) [9], clipping and filtering [10], coding [11], partial transmit sequence (PTS) [12, 13] and interleaving [14] were suggested in the literature.

In case of considering the aforementioned classical PAPR reduction algorithms given in [5-14], SLM technique takes part in the most prominent ones with its significant PAPR reduction capability. The SLM technique provides an efficient and distortionless PAPR reduction by multiplying the original quadrature amplitude modulation (QAM) modulated data sequence with the certain number of alternative phase rotation factor combinations to generate different candidate signals to be transmitted and picking the one with minimal PAPR for transmission [7, 8]. In this study, the SLM technique which was primarily suggested for the conventional OFDM was flawlessly applied to the UPMC waveform.

Some of the works handling the PAPR issue in the UPMC signal are as follows [15-18]: Baig et al. [15] embedded a type of linear precoder based on discrete Hartley transform to the transmitter side of the UPMC scheme to eliminate its PAPR problem. Taşpınar and Şimşir [16] suggested a practical and effective way of implementing PTS-based PAPR alleviation in the UPMC transmitter. In the related paper, they gave detailed mathematical expressions clarifying the operations performed in the PAPR minimization process. Tipan et al. [17] compared some types of clipping techniques to each other on the basis of their achievements on the amount of PAPR improvement in the UPMC transmission signal. In the same paper, an investigation regarding how much effect each of the related clipping methods has on the BER results of the UPMC waveform was also carried out. Rong et al. [18] applied the PTS to the UPMC waveform in a high complex manner and the complexity of the related application was reduced without causing almost any performance lost in the PAPR reduction process.

The outline of our paper is as follows: In Section 2, the acquisition of UPMC signal was described and the PAPR definition of the related signal was given. In Section 3, the PAPR improvement using SLM technique in the UPMC waveform was explained in detail. In Section 4, the simulation results were investigated and at last, the article was finished by yielding the conclusions of our study in Section 5.

## 2. UPMC Signal Acquisition and PAPR Definition

The UPMC signals are produced by fulfilling the transmitter operations demonstrated in Figure 1 via the block diagram [1-4].

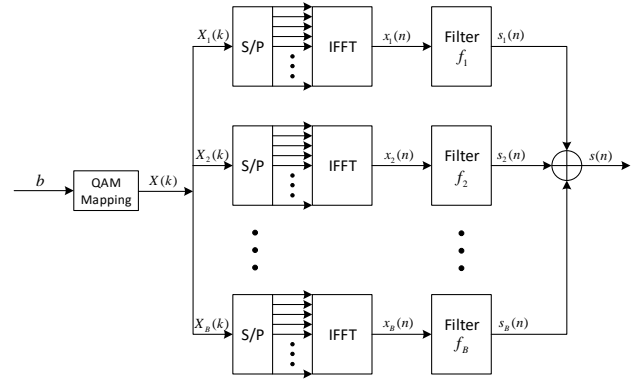


Figure 1. Signal generation at the UPMC transmitter

As clearly understood from the Figure 1, the UPMC transmitter operations start with modulating the information bits by the QAM modulator. Then the QAM symbols obtained from the modulator output is allocated to the certain positions in the multiple sub-bands that are acquired by dividing the whole band into the multiple parts with certain sizes. Subsequent to the inverse fast Fourier transform (IFFT) operation performed on each symbol group, the time domain signal belonging to the  $b$ th sub-band is obtained as follows [16]:

$$x_b(n) = \frac{1}{\sqrt{N}} \sum_{k=0}^{N-1} X_b(k) e^{j2\pi kn/N} \quad (1)$$

$$; 0 \leq n \leq N-1; \quad 1 \leq b \leq B$$

In Equation (1),  $X_b(k)$  represents the  $b$ th sub-band frequency domain signal.  $N$ ,  $k$  and  $B$  denote the subcarrier number, subcarrier indices and the total sub-band number, respectively. Following the operation of cyclic prefix to the time domain signals  $x_b(n)$ , the related signals are filtered one by one through the finite impulse response (FIR) filters and then added together to generate the UPMC signal specified by  $s(n)$ . Hereby, the PAPR definition of the time domain signal acquired from the UPMC transmitter output is expressed in the following manner [16]:

$$PAPR(dB) = 10 \log_{10} \frac{\max_{0 \leq n \leq N+L_{CP}+L_f-1} |s(n)|^2}{E[|s(n)|^2]} \quad (2)$$

where  $L_{CP}$  and  $L_f$  represent the lengths of cyclic prefix and FIR filter, respectively.

## 3. SLM-Based PAPR Improvement in UPMC Signal

Our way of applying the SLM technique [7, 8] to the UPMC transmitter was expressed visually in Figure 2. As demonstrated in Figure 2, in the first instance, the

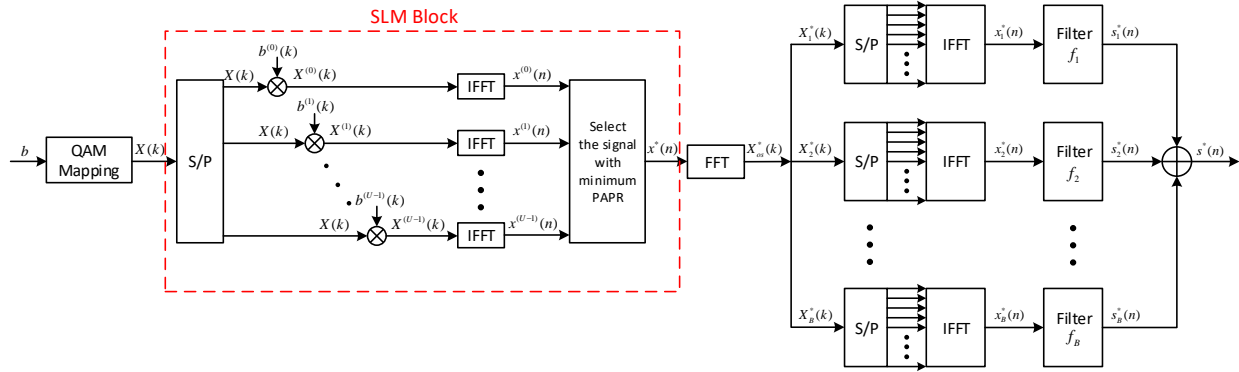


Figure 2. The block diagram of PAPR reduction process employing SLM technique in the UPMC waveform

information data acquired from the output of QAM modulator is given to the input of SLM block. The signals optimized by the SLM algorithm are then subjected to the fast Fourier transform (FFT) process in order to make the related signals suitable for being applied to the UPMC transmitter input. The frequency domain data sequence acquired from the output of FFT block are given to the input of UPMC transmitter. Finally, the signals achieved from the UPMC transmitter output will possess the minimized PAPR values. The operations performed for achieving the UPMC signal with minimum PAPR employing the SLM technique are clarified below:

At first, the information bits are subjected to any type of QAM modulation and in consequence of this, the following data sequence consisting of QAM symbols is obtained:

$$X(k) = [X(0), X(1), \dots, X(N-1)] \quad (3)$$

The sequence of  $X(k)$  is then multiplied by the  $N$  length alternative phase rotation factor sequences  $b^{(u)}(k) = [b^{(u)}(0), b^{(u)}(1), \dots, b^{(u)}(N-1)]$  generated randomly where  $b^{(u)}(k) \in \{1, -1\}$ ,  $u = 0, 1, \dots, U$ .  $U$  specifies the number of randomly generated phase factor combinations. Following the multiplication process, the phase rotated data sequence denoted by  $X^{(u)}(k)$  can be expressed as follows:

$$X^{(u)}(k) = [X(0) \cdot b^{(u)}(0), X(1) \cdot b^{(u)}(1), \dots, X(N-1) \cdot b^{(u)}(N-1)] \\ = [X^{(u)}(0), X^{(u)}(1), \dots, X^{(u)}(N-1)] \quad (4)$$

Later on,  $X^{(u)}(k)$  is oversampled via the zero padding process in which  $(L-1)N$  zeros are inserted into the related  $N$  length sequence:

$$X_{os}^{(u)}(k) = \left[ \underbrace{0, 0, \dots, 0}_{(L-1)N/2}, \underbrace{X^{(u)}(0), X^{(u)}(1), \dots, X^{(u)}(N-1)}_N, \underbrace{0, 0, \dots, 0}_{(L-1)N/2} \right] \quad (5)$$

where  $L$  corresponds to the oversampling factor. The oversampled phase rotated data vector is subjected to the IFFT operation to attain the following signal in time domain:

$$x^{(u)}(n) = IFFT(X_{os}^{(u)}(k)) \\ = \frac{1}{\sqrt{N}} \sum_{k=0}^{N-1} X(k) \cdot b^{(u)}(k) \cdot e^{\frac{j2\pi kn}{LN}}, \quad 0 \leq n \leq LN-1 \quad (6)$$

The optimum phase rotation combination  $b^*(k)$  minimizing the PAPR of  $x^{(u)}(n)$  signal can be found as follows:

$$b^*(k) = \arg \min_{b^{(u)}(k)} \left\{ \max_{0 \leq n \leq LN-1} \left| \frac{1}{\sqrt{N}} \sum_{k=0}^{N-1} X(k) \cdot b^{(u)}(k) \cdot e^{\frac{j2\pi kn}{LN}} \right|^2 \right\} \quad (7)$$

where the  $\arg \min \{ \}$  operator finds the optimum  $b^{(u)}(k)$  minimizing the value of expression in the brackets. Subsequent to finding the optimum phase rotation sequence  $b^*(k)$ , the optimized signal in time domain is acquired from the SLM output in the following way:

$$x^*(n) = \frac{1}{\sqrt{N}} \sum_{k=0}^{N-1} X(k) \cdot b^*(k) \cdot e^{\frac{j2\pi kn}{LN}}, \quad 0 \leq n \leq LN-1 \quad (8)$$

After that,  $x^*(n)$  is subjected to the FFT operation for being able to be used as an input data sequence in the UPMC transmitter.  $X_{os}^*(k)$  data sequence acquired from the FFT output corresponds to the zero inserted frequency

domain optimal data sequence  $X^*(k)$  which is equal to the multiplication of  $X(k)$  by the optimum phase factor combination  $b^*(k)$ . After the FFT process, the resulting data vector  $X_{os}^*(k)$  is allocated to  $B$  sub-bands. The frequency domain data sequence belonging to the sub-band  $b$  is denoted by  $X_b^*(k)$ . Subsequent to fulfilling the next operation which is performing the IFFT process for every sub-band, two more operations called cyclic prefix and filtering are applied to the time domain signal  $x_b^*(n)$ , respectively and after that, the resulting signals on the multiple sub-bands are combined. Finally, the optimal UFGC signal denoted by  $s^*(n)$  with minimized PAPR is acquired from transmitter end. Exhaustive mathematical expressions of the operations performed after the acquisition of  $x^*(n)$  to achieve the  $s^*(n)$  can be found from [16].

#### 4. Simulation Results

The SLM technique initially suggested for the OFDM was optimally integrated to the transmitter of UFGC scheme in order to get the maximum PAPR reduction performance from the related technique. In the simulations, the efficiency of SLM scheme on minimizing the PAPR of UFGC waveform was analyzed for varied number of phase sequence vectors each of which are generated in a random way. The complementary cumulative distribution function (CCDF =  $\Pr[ \text{PAPR} > \text{PAPR}_0 ]$ ) was utilized in the simulations for the analysis of PAPR reduction achievement. Following the analyses made on the PAPR improvements achieved in the UFGC signal, the effect of SLM technique on the level of side lobes and BER belonging to the UFGC signal amplified by one of the most commonly used nonlinear HPAs called solid state power amplifier (SSPA) [19], was investigated for various SLM and SSPA parameters such as the number of randomly generated phase factor combinations ( $U$ ), input back off (IBO) value and the value of smoothness ( $p$ ) coefficient. The parameters appointed for the simulations are yielded in Table 1.

In Figure 3, an investigation on the SLM's ability to reduce the PAPR of UFGC signal was carried out for various number of phase sequences. Figure 3 clearly demonstrates that the PAPR of original UFGC signal can be reduced significantly by increasing the value of  $U$ . For instance, since the performance of SLM technique escalates with the increase in the number of alternative phase sequences, the enhancement in the value of  $U$  from 4 to 256 provides 5.8 dB PAPR improvement at CCDF =  $10^{-3}$ .

Table 1. Simulation parameters

Number of subcarriers	32
Type of modulation	4-QAM
Value of oversampling factor	$L=8$
Size of FFT	256
Number of sub-band	2
Type of filter	Dolph-Chebyshev
Length of cyclic prefix	$L_{CP}=16$
Frequency of sampling	3.84 MHz
Type of HPA	SSPA
Type of channel	AWGN

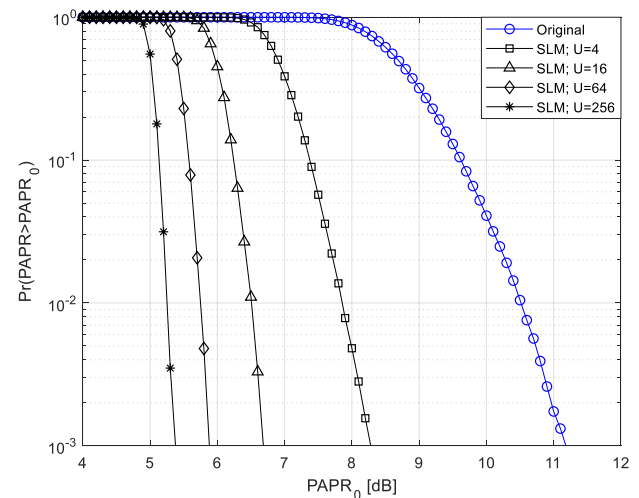


Figure 3. The PAPR improvements achieved by the SLM scheme for different values of  $U$

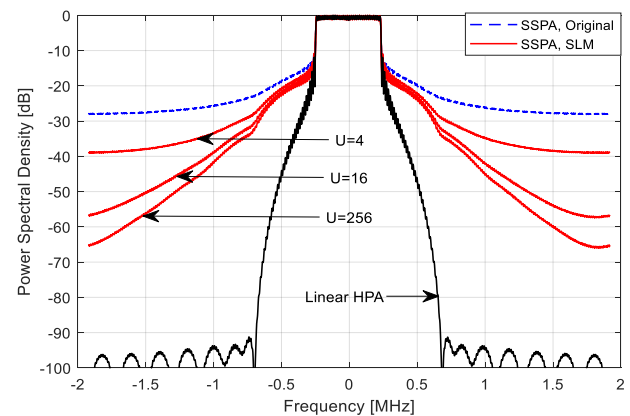


Figure 4. The performance of SLM technique on suppressing the SSPA originated side lobe escalation in the UFGC waveform for several  $U$  values (IBO = 7,  $p = 1$ )

In Figure 4, the SLM performance on suppressing the side lobe escalation arisen from the usage of SSPA for amplifying the UFGC signal with high PAPR before the transmission process, was analyzed via the power spectral density (PSD) graph for several  $U$  values. As can be seen from the Figure 4, the side lobes of the original UFGC

signal were reduced from above the level of  $-30$  dB to approximately  $-65$  dB by enhancing the value of  $U$  from 4 to 256. Since the signals with high PAPR are exposed to nonlinear amplification originated distortion by the SSPA, reducing the signal PAPR through the SLM technique leads to less distortion while amplifying the signal and consequently, high level side lobes arisen from the signal distortions are reduced as well.

In Figure 5, the capability of the SLM procedure was evaluated with regard to its effect on the BER of the UPMC waveform for several IBOs. As distinctly viewed from the Figure 5, for each of the IBO values determined for this simulation, in case of increasing the number of phase sequences, the PAPR of UPMC is further improved and depending on this, the amplification of the related

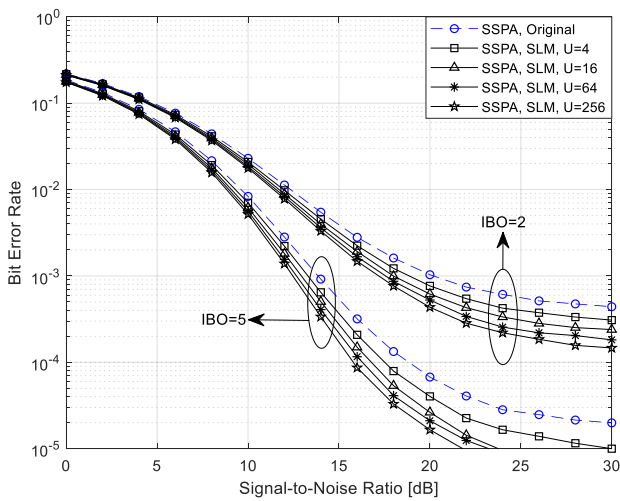


Figure 5. Performance of SLM procedure on reducing the SSPA originated BER increase in the UPMC waveform for different IBO values ( $p = 2$ )

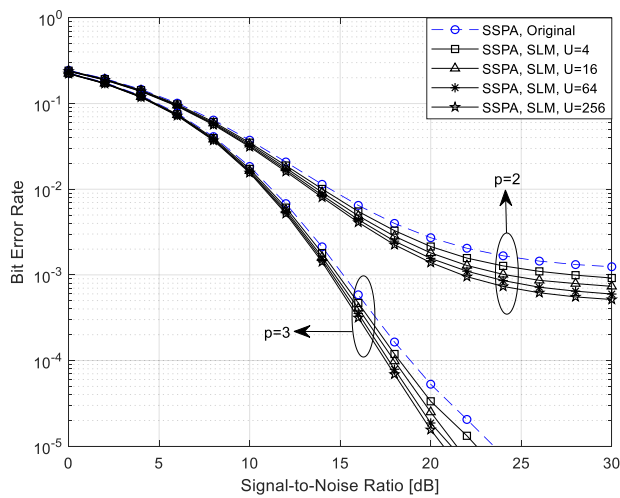


Figure 6. Performance of SLM scheme on reducing the SSPA originated BER increase in the UPMC waveform for different smoothness values ( $IBO = 0$ )

signal via the SSPA is carried out with less degradation which results in a significant improvement in the BER performance. For instance, if the BER results at 20 dB signal-to-noise ratio (SNR) value for  $IBO = 5$  dB are taken into consideration, the BER values achieved for 4, 16, 64 and 256 phase sequences are equal to  $4 \times 10^{-5}$ ,  $2.64 \times 10^{-5}$ ,  $2.1 \times 10^{-5}$  and  $1.66 \times 10^{-5}$ , respectively while the BER of the original signal is equal to  $6.75 \times 10^{-5}$ . Apart from this, increasing the value of IBO corresponding to the parameter that determines the distance of the operating point to the threshold value beyond which the SSPA reaches the saturation, gives rise to BER improvement in the UPMC waveform since the frequency of reaching the saturation region leading to signal distortions during the amplification process decreases.

In Figure 6, the BER graph of the UPMC waveform utilizing the SLM technique for PAPR reduction was obtained with respect to the varied smoothness values. As can be easily realized from the Figure 6, the value of BER belonging to the UPMC waveform scales down with the increase in the number of alternative phase factor combinations generated for minimizing the PAPR of transmission signal. Besides, the enhancement in the value of smoothness coefficient symbolized by  $p$  escalates the linearity of SSPA. With an increased linearity of SSPA, the amount of degradation on the signals during the amplification process decreases and depending on this, a significant BER decrement occurs in the UPMC waveform. For instance, with the increase of coefficient  $p$  from 2 to 3, the BERs acquired by the SLM scheme for 4, 16, 64 and 256 phase sequences at 20 dB SNR value decrease from  $2.14 \times 10^{-3}$ ,  $1.81 \times 10^{-3}$ ,  $1.56 \times 10^{-3}$  and  $1.39 \times 10^{-3}$  to  $3.34 \times 10^{-5}$ ,  $2.5 \times 10^{-5}$ ,  $1.87 \times 10^{-5}$  and  $1.56 \times 10^{-5}$ , respectively.

### 5. Conclusions

In this paper, optimal integration of SLM technique initially suggested for OFDM was carried out in order to exploit full of its potential PAPR alleviation capability in the UPMC waveform. The amount of PAPR improvement carried out by the SLM scheme was demonstrated via the  $PAPR_0 - CCDF(Pr[ PAPR > PAPR_0])$  graph in the simulations. From the related graph, the probability that the PAPR of the signal taken from the output of UPMC transmitter is greater than a certain PAPR value ( $PAPR_0$ ) can be easily seen. Besides, the capability of SLM strategy on lowering the SSPA originated spectral regrowth and BER increase was evaluated for different values of  $U$ ,  $IBO$  and  $p$  via the PSD and BER graphs, respectively. The simulation results obviously demonstrates that it is possible to achieve serious improvements through the SLM technique in the PAPR, spectral characteristic and BER performance of the UPMC waveform.

## Declaration

The author(s) declared no potential conflicts of interest with respect to the research, authorship, and/or publication of this article. The author(s) also declared that this article is original, was prepared in accordance with international publication and research ethics, and ethical committee permission or any special permission is not required.

## Acknowledgment

This study was supported by the Scientific Research Projects Coordination Unit of Erciyes University [Grant No: FDK-2018-8463].

## References

- Vakilian, V., T. Wild, F. Schaich, S.T. Brink, and J.F. Frigon, *Universal-filtered multi-carrier technique for wireless systems beyond LTE*, in GC Wkshps 2013: Atlanta. p. 223-228.
- Li, Y., B. Tian, K. Yi, and Q. Yu, *A novel hybrid CFO estimation scheme for UFMC-based systems*. IEEE Communications Letters, 2017. **21**(6): p. 1337-1340.
- Wu, M., J. Dang, Z. Zhang, and L. Wu, *An advanced receiver for universal filtered multicarrier*. IEEE Transactions on Vehicular Technology, 2018. **67**(8): p. 7779-7783.
- Duan, S., X. Yu, and R. Wang, *Performance analysis on filter parameters and sub-bands distribution of universal filtered multi-carrier*. Wireless Personal Communications, 2017. **95**(3): p. 2359-2375.
- Chen, J.C. and C.K. Wen, *PAPR reduction of OFDM signals using cross-entropy-based tone injection schemes*. IEEE Signal Processing Letters, 2010. **17**(8): p. 727-730.
- Krongold, B.S. and D.L. Jones, *PAR reduction in OFDM via active constellation extension*. IEEE Transactions on Broadcasting, 2003. **43**(3): p. 258-268.
- Bauml, R.W., R.F.H. Fischer, and J.B. Huber, *Reducing the peak-to-average power ratio of multicarrier modulation by selected mapping*. Electronics Letters, 1996. **32**(22): p. 2056-2057.
- Wang, C.L. and Y. Quyang, *Low-complexity selected mapping schemes for peak-to-average power ratio reduction in OFDM systems*. IEEE Transactions on Signal Processing, 2005. **53**(12): p. 4652-4660.
- Liang, H., H.C. Chu, and C.B. Lin, *Peak-to-average power ratio reduction of orthogonal frequency division multiplexing systems using modified tone reservation techniques*. International Journal of Communication Systems, 2016. **29**(4): p. 748-759.
- Li, X. and L.J. Cimini, *Effect of clipping and filtering on the performance of OFDM*. IEEE Communications Letters, 1998. **2**(5): p. 131-133.
- Jones A.E., T.A. Wilkinson, and S.K. Barton, *Block coding scheme for reduction of peak to mean envelope power ratio of multicarrier transmission scheme*. Electronics Letters, 1994. **30**(25): p. 2098-2099.
- Cimini, L.J. and N.R. Sollenberger, *Peak-to-average power ratio reduction of an OFDM signal using partial transmit sequences*. IEEE Communications Letters, 2000. **4**(3): p. 86-88.
- Bozkurt, Y.T. and N. Taşpınar, *PAPR reduction performance of bat algorithm in OFDM systems*. International Advanced Researches and Engineering Journal, 2019. **3**(3): p. 150-155.
- Jayalath, A.D.S. and C. Tellambura, *Reducing the peak-to-average power ratio of orthogonal frequency division multiplexing signal through bit or symbol interleaving*. Electronics Letters, 2000. **36**(13): p. 1161-1163.
- Baig, I., U. Farooq, N.U. Hasan, M. Zghaibeh, A. Sajid, and U.M. Rana, *A low PAPR DHT precoding based UFMC scheme for 5G communication systems*, CoDIT 2019: Paris. p. 425-428.
- Taşpınar, N. and Ş. Şimşir, *PAPR reduction based on partial transmit sequence technique in UFMC waveform*, in CISTI 2019: Coimbra. p. 1-6.
- Tipan, M.N., J. Caceres, M.N. Jimenez, I.N. Cano, and G. Arevalo, *Comparison of clipping techniques for PAPR reduction in UFMC systems*, LATINCOM 2017: Guatemala City. p. 1-4.
- Rong, W., J. Cai, and X. Yu, *Low-complexity PTS PAPR reduction scheme for UFMC systems*. Cluster Computing, 2017. **20**(11): p. 3427-3440.
- Ryu, H.G., J.S. Park, and J.S. Park, *Threshold IBO of HPA in the predistorted OFDM communication system*. IEEE Transactions on Broadcasting, 2004. **50**(4): p. 425-428.